Jpn. J. Appl. Phys. Vol. 40 (2001) pp. 2092–2094
Part 1, No. 3B, March 2001
©2001 The Japan Society of Applied Physics

Photoluminescence Dynamics of CdS Nanocrystals Fabricated by Sequential Ion Implantation

Daisuke MATSUURA[1], Yoshihiko KANEMITSU[1,*], Takashi KUSHIDA[1], Clark W. WHITE[2], John D. BUDAI[2] and Alkiviathes MELDRUM[3]

[1]*Graduate School of Materials Science, Nara Institute of Science and Technology, Ikoma, Nara 630-0101, Japan*
[2]*Solid State Division, Oak Ridge National Laboratory, Oak Ridge, Tennessee 37831, USA*
[3]*Department of Physics, The University of Alberta, Edmonton, Alberta T6G 2J1, Canada*

(Received September 5, 2000; accepted for publication October 26, 2000)

We have studied photoluminescence (PL) dynamics of CdS nanocrystals fabricated by sequential Cd^+ and S^+ ion implantation into Al_2O_3 matrices. The PL spectrum and PL decay dynamics of CdS nanocrystals are sensitive to the measurement temperature. This is because excitons trapped at shallow localized states are thermally excited to the high-energy state at high temperatures. Two PL bands appear near the absorption edge at elevated temperatures near 100 K. From time-resolved PL spectra and the PL decay dynamics, it is concluded that the observed PL bands near the absorption edge are due to free excitons and excitons trapped at shallow localized states. The PL mechanism in CdS nanocrystals is discussed.

KEYWORDS: nanocrystal, exciton, CdS, ion implantation, photoluminescence

1. Introduction

Recently, there is intense interest in physical properties of semiconductor nanocrystals because they exhibit strongly size-dependent optical and electrical properties and these behaviors open new applications including high performance optoelectronic devices.[1,2] A variety of semiconductor nanocrystals have been synthesized by many different techniques.[1] One of the most versatile techniques for forming nanocrystals involves high-dose ion implantation followed by thermal annealing.[3] In this method, almost any ion can be implanted into any solid substrate and thermal annealing leads to precipitation of nanocrystals from supersaturated solid solutions. Ion implantation and thermal annealing can be used to create semiconductor nanocrystals embedded in the near surface of transparent matrices such as SiO_2 and Al_2O_3. Furthermore, the synthesis of compounds by sequential ion implantation of the individual constituents is a simple method to produce compound nanocrystals. II-VI and III-V compound semiconductor nanocrystals have been formed in transparent matrices by sequential ion implantation.[3–6] These embedded nanocrystal structures have some advantages and offer attractive options such as the chemical and mechanical stability and applications to optical waveguides and photonic devices. However, ion implantation often introduces structural damage in host materials. The optical characterization of nanocrystals/matrix composite systems is very important for evaluation of crystal quality and device applications of nanocrystals.

In this work, we have studied the photoluminescence (PL) decay dynamics of CdS nanocrystals. At elevated temperatures, the thermal excitation rate from the localized to the free-exciton states determines the PL spectrum and dynamics.

2. Experimental

The c-axis oriented single crystal α-Al_2O_3 was used as a host material in this work. Equal doses ($4.3 \times 10^{16}/cm^2$) of Cd^+ (at 450 keV) and S^+ (at 164 keV) were implanted into the substrates at 600°C, and then the samples were annealed in flowing 96% Ar+4% H_2 to induce precipitation and nanocrystal formation. In isochronal and isothermal annealing experiments, the highest PL intensity under 3.10 eV laser excitation was observed in the sample annealed at 1000°C for 60 min. In this work, we study the PL dynamics of this sample annealed at 1000°C for 60 min. X-ray diffraction and transmission electron microscopy[7,8] showed that CdS nanocrystals have the wurtzite structure and the average diameter was ~17 nm. Time-resolved PL spectra were measured using a streak camera under frequency-doubled picosecond Ti:Al_2O_3 laser excitation.

3. Results and Discussion

Figure 1 shows absorption and PL spectra of CdS nanocrystals at 5, 50, and 100 K. Two exciton-related peaks[9,10] appear in the absorption spectrum and the PL band appears near the absorption edge. With increasing temperature, the spectral shape of the PL band becomes complicated. At elevated temperatures near 100 K, three bands, E_a, E_b, and E_c indicated in Fig. 1, appear in the PL spectrum. The energy position of the highest-energy peak at 100 K is higher than that of the main peak at 5 K, although the lowest absorption peak gradually shifts to lower energy with an increase of temperature.[10] Therefore, it is speculated that at elevated temperatures excitons localized at lower states are thermally excited to upper states and a new and high-energy band, E_a, appears in the PL spectrum. In order to clarify the origin of the PL bands near the absorption edge, we measured picosecond time-resolved PL spectra of CdS nanocrystals in Al_2O_3 matrices under 3.10 eV and 1.8-ps laser excitation.

Figure 2 shows PL decay curves monitored at 2.58, 2.48 and 2.36 eV for CdS nanocrystals embedded in Al_2O_3 at 33 K. These emission energies correspond to the three PL bands in Fig. 1. At 2.58 eV, the PL intensity rapidly decreases within 10 ns, while at 2.36 eV, the PL intensity gradually decreases up to the microsecond time region. At 2.48 eV, the PL decay profile consists of two components: the fast-decay component (<10 ns) and the slow-decay component (several hundreds of nanoseconds). The fast-decay component is dominant at the high-energy emission, while the slow component at the low-energy emission region. The PL band near the absorption

*Author to whom all correspondence should be addressed; E-mail address: sunyu@ms.aist-nara.ac.jp

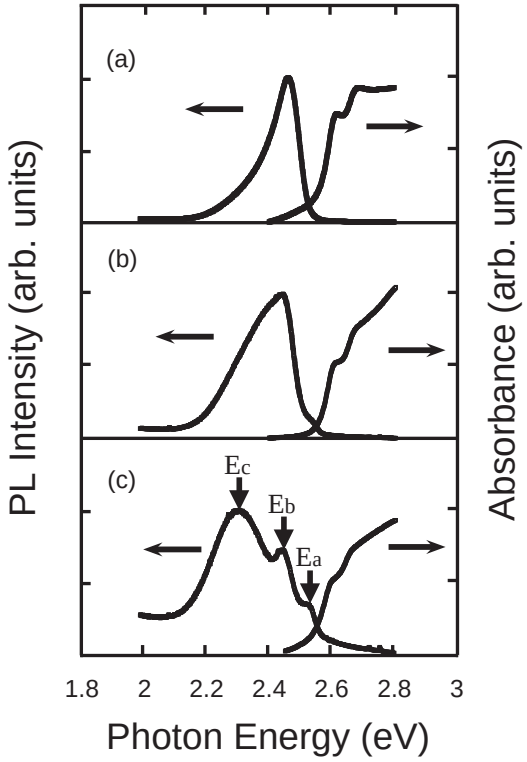

Fig. 1. Optical absorption and PL spectra of CdS nanocrystals embedded in Al_2O_3 at (a) 5, (b) 50, and (c) 100 K. Three PL bands, E_a, E_b, and E_c, clearly appear in the PL spectrum at elevated temperatures near 100 K.

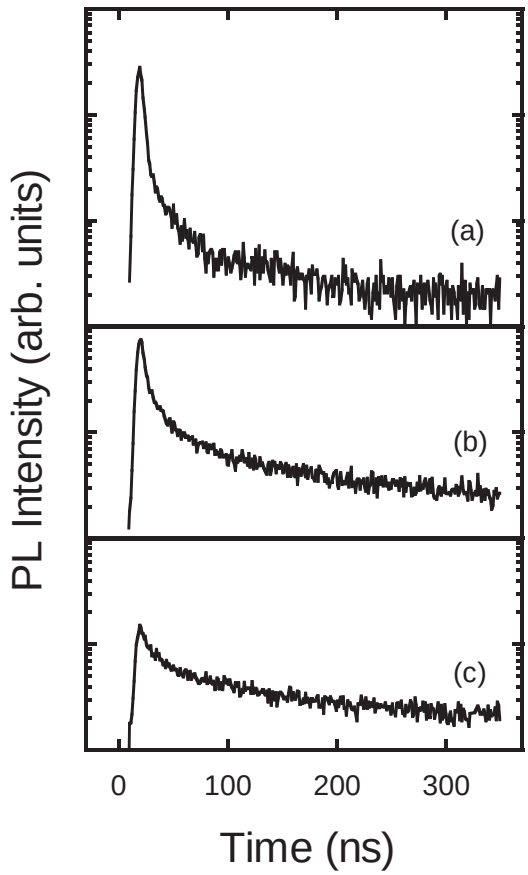

Fig. 2. PL decay curves of CdS nanocrystals embedded in Al_2O_3 at (a) 2.58, (b) 2.48, and (c) 2.36 eV at 33 K.

edge shows fast decay and the E_c band of Fig. 1 shows slow decay.

It is considered that the slow component is related to excitons localized at impurities or defects in CdS nanocrystals. In our fabrication method, CdS nanocrystals may contain Al impurities. The energy difference between the highest PL peak, E_a, and the lowest PL peak, E_c, is about 200 meV. This value is in fairly good agreement with the energy difference between the valence band and the Al acceptor level in the Al-doped CdS crystals.[11] Therefore, it is concluded that the broad E_c band is attributed to excitons bound to Al impurities in CdS nanocrystals and the PL lifetime of excitons bound to Al impurities is several hundred nanoseconds. Hereafter, we focus on discussion of the origin of the E_a and the E_b bands of Fig. 1 near the absorption edge.

Figure 3 shows optical absorption and time-resolved PL spectra of CdS nanocrystals in Al_2O_3 matrices at 10, 50, and 100 K. The PL spectra integrated from 0 ps to 1 ns are shown in this figure. At low temperatures, an asymmetric PL band is observed near the absorption edge. At higher temperatures (>30 K), the PL band consists of two components. There is no essential Stokes shift between the lowest-absorption peak and the higher-energy PL peak. In addition, the temperature dependence of the E_a peak energy is consistent with that of the lowest-absorption peak (A-exciton peak in wurtize CdS).[10] Therefore, it is considered that the higher-energy E_a band is due to free-exciton emission and the lower-energy E_b to the exciton localized at shallow states. The three PL bands shown in Fig. 1 mean the free exciton (E_a), the exciton trapped at shallow localized states (E_b), and the exciton bound to Al acceptor state (E_c). At elevated temperatures the bound exciton at shallow localized states is thermally excited to the free exciton state and then the free exciton emission is clearly observed.

Figure 4 shows PL dynamics of the fast-decay component at the two peak energies of time-resolved PL spectra at 25 and 100 K. These monitored photon energies of 2.50 and 2.57 eV correspond to two peaks in Fig. 3. The PL decay profiles, $I(t)$, can be fitted by two single-exponential functions,

$$I(t) \approx I_1 \exp(-t/\tau_1) + I_2 \exp(-t/\tau_2), \qquad (1)$$

where I_1 and I_2 are the PL intensities just after the pulsed laser excitation and τ_1 and τ_2 are time constants. The τ_1 (short) component (<200 ps) is ascribed to the free excitons in CdS nanocrystals.[10] It is speculated that the τ_2 (long) component (~2 ns) is due to the excitons at shallow localized states. With increasing temperature, the I_2/I_1 ratio at the higher-energy emission (Fig. 4(a)) gradually decreases, while the I_2/I_1 ratio at the lower-energy emission (Fig. 4(b)) rapidly decreases.

After the short-pulse laser excitation, free excitons will be created first from photo-generated electron-hole pairs in CdS nanocrystals. Then, the free-exciton population decreases rapidly by the trapping to impurities and defects as well as by radiative and nonradiative recombinations. The short decay-time component in Fig. 4(a) is considered to be due to these free excitons. Excitons bound to shallow states are thermally excited to the free-exciton state. Since the lifetime of free excitons is much shorter than that of localized exciton states, the time behavior of the population of excitons at shallow localized states determines the PL decay dynamics after the first several hundred picoseconds. The gradual decrease in the I_2/I_1 intensity ratio with increasing temperature in Fig. 4(a) is explained by the increase in the thermal excitation rate of bound excitons. At the peak of the E_b band, there is no contri-

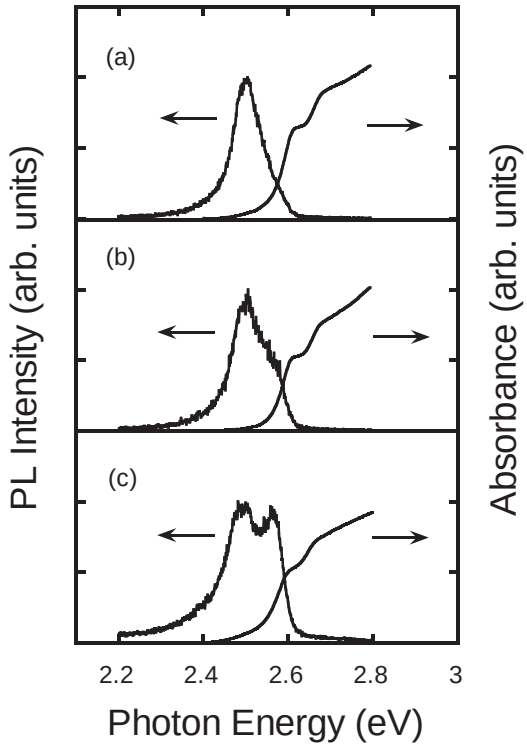

Fig. 3. Optical absorption and time-resolved PL spectra of CdS nanocrystals embedded in Al_2O_3 at (a) 10, (b) 50, and (c) 100 K. PL spectra integrated from 0 ps to 1 ns are shown.

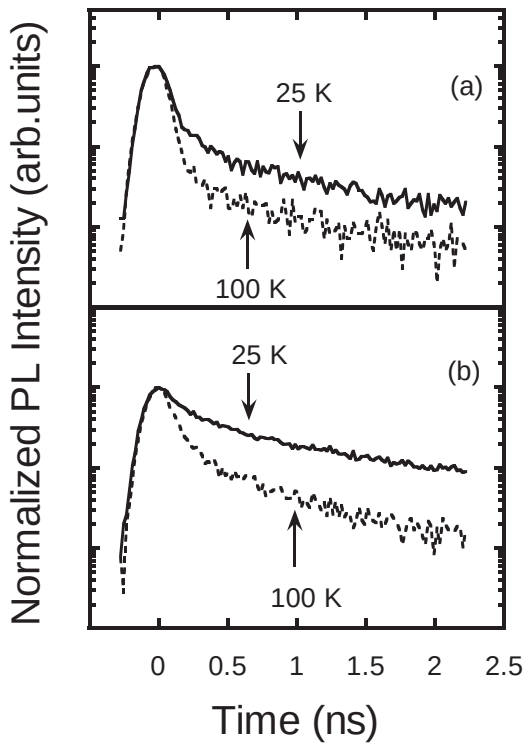

Fig. 4. PL decay curves at 25 and 100 K at (a) 2.57 and (b) 2.50 eV.

bution of free-exciton emission at very low temperatures. The free-exciton emission line broadens with temperature, and the free-exciton emission is observed around 2.50 eV at elevated temperatures around 100 K. This explains the increase in the I_1/I_2 ratio with increasing temperature in Fig. 4(b).

From the temperature dependence of time-resolved PL spectra, it is concluded that the observed PL bands near the absorption edge are due to the free-exciton emission and bound exciton emission at shallow localized states. The thermal excitation of excitons from localized states to the free exciton state plays a significant role the PL decay dynamics. Further experimental and theoretical studies are needed for the quantitative understanding of the exciton dynamics in CdS nanocrystals.

4. Conclusion

We have fabricated CdS nanocrystals by Cd^+ and S^+ implantation in Al_2O_3 matrices and studied their exciton dynamics by means of time-resolved PL measurements. At low temperatures, a PL band is observed due to excitons localized at shallow states. At high temperatures, excitons trapped at shallow localized states are thermally excited to the free-exciton state. The free-exciton emission and the trapped exciton emission appear in the PL spectrum near the absorption edge.

Acknowledgements

The authors would like to thank Dr. M. Ando for stimulating discussions. Part of this work at Nara was supported by a Grant-in-Aid of Scientific Research B from Japan Society for the promotion of Science (No. 11440095), The Corning Research Grant Award, Yazaki Memorial Foundation for Science and Technology, and Hosokawa Powder Technology Foundation. Oak Ridge National Laboratory is managed by UT-Battelle, LLC for the U. S. Department of Energy under contract DE-AC05-00OR22725.

1) J. Lumin. **76** (1996) 1–484.
2) MRS Bull. **23** (1998) No. 2, 15–53.
3) C. W. White, J. D. Budai, S. P. Withrow, J. G. Zhu, E. Sonder, R. A. Zuhr, A. Meldrum, D. M. Hembree, Jr. D. O. Henderson and S. Prawer: Nucl. Instrum. & Methods B **141** (1998) 228.
4) J. D. Budai, C. W. White, S. P. Withrow, M. F. Chisholm, J. G. Zhu and R. A. Zuhr: Nature **390** (1997) 384.
5) S. Okamoto, Y. Kanemitsu, K. S. Min and H. A. Atwater: Appl. Phys. Lett. **73** (1998) 1829.
6) Y. Kanemitsu, H. Tanaka, Y. Fukunishi, T. Kushida, K. S. Min and H. A. Atwater: Phys. Rev. B **62** (2000) 5100.
7) A. Meldrum, C. W. White, L. A. Boatner, I. M. Anderson, R. A. Zuhr, E. Sonder, J. D. Budai and D. O. Henderson: Nucl. Instrum. & Methods B **148** (1999) 957.
8) A. Meldrum, E. Sonder, R. A. Zuhr, I. M. Anderson, J. D. Budai, C. W. White, L. A. Boatner and D. O. Henderson: J. Mater. Res. **14** (1999) 4489.
9) A. Anedda and E. Fortin: Phys. Status Solidi (a) **36** (1976) 385.
10) D. Matsuura, Y. Kanemitsu, T. Kushida, C. W. White, J. D. Budai and A. Meldrum: Appl. Phys. Lett. **77** (2000) 2289.
11) N. Susa, H. Watanabe and M. Wada: Jpn. J. Appl. Phys. **14** (1975) 1733.